

# RSC Advances

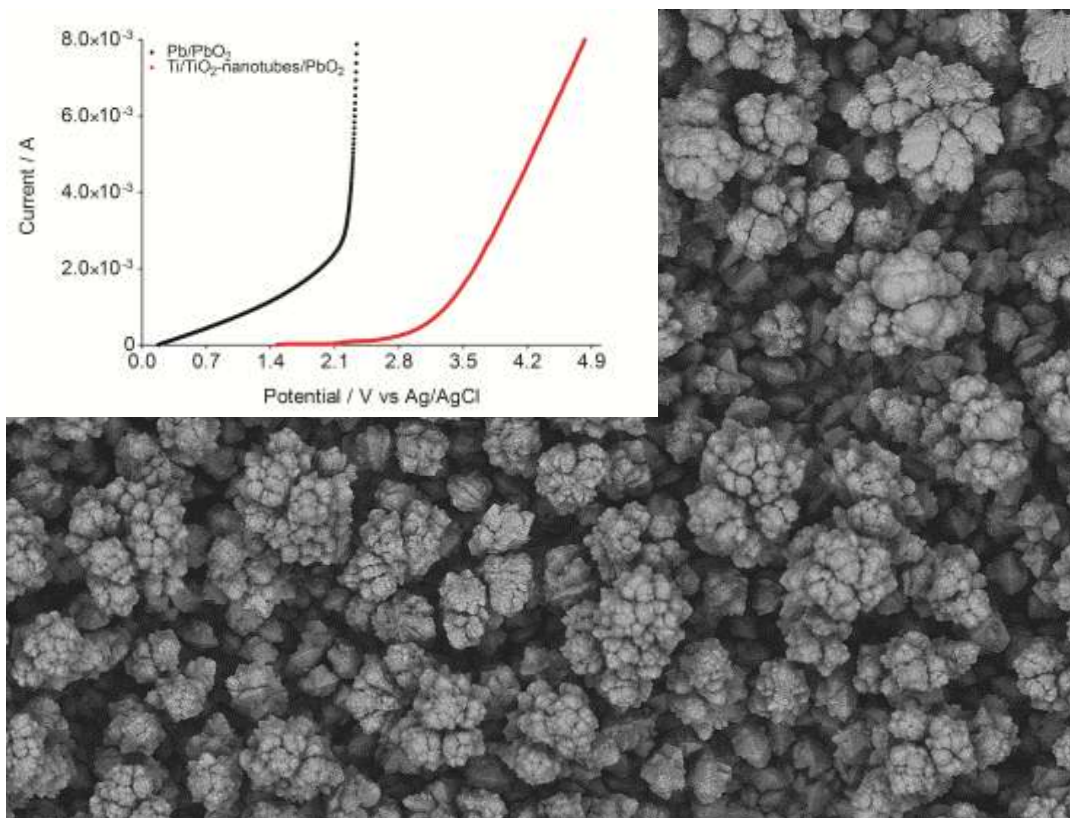


This is an *Accepted Manuscript*, which has been through the Royal Society of Chemistry peer review process and has been accepted for publication.

*Accepted Manuscripts* are published online shortly after acceptance, before technical editing, formatting and proof reading. Using this free service, authors can make their results available to the community, in citable form, before we publish the edited article. This *Accepted Manuscript* will be replaced by the edited, formatted and paginated article as soon as this is available.

You can find more information about *Accepted Manuscripts* in the [Information for Authors](#).

Please note that technical editing may introduce minor changes to the text and/or graphics, which may alter content. The journal's standard [Terms & Conditions](#) and the [Ethical guidelines](#) still apply. In no event shall the Royal Society of Chemistry be held responsible for any errors or omissions in this *Accepted Manuscript* or any consequences arising from the use of any information it contains.



## Large disk electrodes of Ti/TiO<sub>2</sub>-Nanotubes/PbO<sub>2</sub> for environmental applications

Dayanne Chianca de Moura<sup>a</sup>, Mónica Cerro-López<sup>b</sup>, Marco Antonio Quiroz<sup>b</sup>, Djalma Ribeiro da Silva<sup>a</sup> and Carlos Alberto Martínez-Huitle<sup>\*a</sup>

<sup>a</sup> Federal University of Rio Grande do Norte, Institute of Chemistry, Lagoa Nova - CEP 59.072-970, RN, Brazil.

<sup>b</sup> Universidad de las Américas Puebla. Grupo de Investigación en Energía y Ambiente. ExHda. Sta. Catarina Martir s/n, Cholula 72820, Puebla, México.

### Abstract

Large disk electrodes of Ti/TiO<sub>2</sub>-Nanotubes/PbO<sub>2</sub> (65 cm<sup>2</sup> of geometrical area) were successfully synthesized by anodization and electrodeposition procedures. Characterization of anodes was performed by SEM, EDS, AFM and electrochemical measurements, aiming environmental applications. PbO<sub>2</sub> electrocatalytic material promotes the production of strong oxidant species (hydroxyl radicals) that can be used for decontamination. Electrochemical treatment of synthetic dye effluent (2 L) containing with 250 mg L<sup>-1</sup> of Acid Blue 113 dye (AB 113) was performed using a disk Ti/TiO<sub>2</sub>-nanotubes/PbO<sub>2</sub> anode by using electrochemical flow cell. More than 85% of organic matter was removed by applying 20, 40 and 60 mA cm<sup>-2</sup>. Meanwhile, colour decay achieved values of 60, 90 and 100%, depending on the applied current density. Alternatively, this study allows to understand how nanomaterials has avoided the corrosion phenomena on the anode surface (Pb<sup>2+</sup> pollution) due to the homogeneous migration of PbO<sub>2</sub> within the TiO<sub>2</sub> nanotubes previously formed on Ti support.

## Introduction

Lead dioxide coatings on inert substrates such as titanium and carbon now offer new opportunities as anodic material for environmental applications. It is now recognised that electrodeposition allows the preparation of stable coatings with different phase structures and a wide range of surface morphologies.<sup>1</sup> In addition, substantial modification to the physical properties and catalytic activities of the coatings are possible through doping and the fabrication of nanostructured deposits or composites.<sup>1,2</sup> Lead dioxide may be electrodeposited onto inert substrates such as titanium or carbon from a number of media where the Pb(II) is soluble.<sup>2,3</sup> These electrodes can only be used in applications that require a rather positive potential, as electrochemical oxidation (EO). If a positive potential is applied, the coating will be protected from corrosion; but, at any potential significantly negative, cathodic reduction and dissolution of the lead dioxide coating is expected.<sup>4,5</sup> Ti is the usual substrate for PbO<sub>2</sub> coatings even when adhesion is a problem yet.<sup>6-8</sup> Ti usually in the form of a plate or expanded metal mesh, must be pre-treated before the anodic plating process in order to remove existing TiO<sub>2</sub> scale from the surface and roughen the surface and to prevent passivation. This pre-treatment commonly involves, first sandblasting, alkaline degrease followed by etching in heated oxalic acid or HCl for at least 30 min. Several times this pre-treatment may be insufficient, and various thin undercoats on Ti before deposition of the PbO<sub>2</sub> have been proposed—gold, platinum, tin dioxide, TiO<sub>2</sub>/Ta<sub>2</sub>O<sub>5</sub>, PtO<sub>x</sub> and TiO<sub>2</sub>/RuO<sub>2</sub>.<sup>8-12</sup> The main problem is that Ti self-generates an oxide layer that affects several of its properties, such as charge transport and ability to adhere deposits on its surface. However, some research groups have recently developed nanostructured materials<sup>13,14</sup> of TiO<sub>2</sub> such as nanotubes, nanorods and nanowires, as supporting to deposit PbO<sub>2</sub>.<sup>15-17</sup> The unique properties of high aspect ratio of TiO<sub>2</sub> nanotubes include large surface area, high cation

exchangeability, high catalytic activity, easier separation and recyclability.<sup>18</sup> Three popular synthesizing techniques of TiO<sub>2</sub> nanotubes have been investigated in recent years including template-assisted, electrochemical anodization and hydrothermal treatment.<sup>19-24</sup> The method of electrochemical anodization is based on the anodization of titanium foil to obtain nanoporous TiO<sub>2</sub>.<sup>25</sup> Basically, TiO<sub>2</sub> nanotubes grow on the Ti surface with ordered arrangement and high aspect ratio, being controlled by the dimensions of nanotubes formed by applying different electrolyte composition, applied voltage, pH and anodizing time.<sup>26,27</sup> TiO<sub>2</sub> nanotubes electrodes have superior photo-reactivity, non-toxicity, long term stability, high corrosion resistance and available in low cost.<sup>28-30</sup> These features offer a useful way to fabricate nanoscale architectures of metal oxides by using this method. In the case of PbO<sub>2</sub>, it clearly emerges as an attractive material as an anode for the direct oxidation of organic compounds due to its high oxygen evolution potential, low price, relatively stable under the high positive potentials required and stability at high temperatures.<sup>31</sup> The formation and growth of PbO<sub>2</sub> inside TiO<sub>2</sub> nanotubes have been already developed and used for environmental applications, but no significant dimensions of geometrical area have been produced.<sup>32</sup> Therefore, the preparation of more stable PbO<sub>2</sub> anode on a good supporting such as TiO<sub>2</sub> nanotubes could increase the economic value and accelerate the practical applications of these electrocatalytic materials. Herein, we firstly report a general preparation strategy for synthesizing of TiO<sub>2</sub> nanotubes arrays to deposit PbO<sub>2</sub> in order to obtain large-disk electrodes. These synthesized large PbO<sub>2</sub> anodes showed predominant electrochemical performances and are promising tools for the next generation of electrocatalytic materials for environmental applications.

## Experimental

### Preparation of Ti/TiO<sub>2</sub>-nanotubes and Ti/TiO<sub>2</sub>-nanotubes/PbO<sub>2</sub>

All electrochemical deposition experiments were performed with a MINIPA MPL-3305 (São Paulo, Brazil) power supply. TiO<sub>2</sub> nanotubes electrode was prepared according to anodic oxidation method reported by Cerro-Lopez and co-workers.<sup>32</sup> In the electrochemical procedure was used a polished Ti disk with 10 cm diameter (1.8 mm thick and nominal surface area of 63.5 cm<sup>2</sup>). Before anodization of the Ti substrate (0.1 mm thick), the sample was sonicated in acetone, ethanol, and methanol successively, for 15 minutes. Then, the anodizing process was performed using two-electrode system (Ti disk serving as the anode and steel serving as the cathode) in a mixture of glycerol and ultrapure water in a 1.3:1 ratio (v/v) containing 0.5 wt% NaF and 0.2 M Na<sub>2</sub>SO<sub>4</sub> as support electrolyte by applying 30 V for 2 h (Fig. S1 of Electronic supplementary information (ESI)). After this procedure, the Ti/TiO<sub>2</sub>-nanotubes disk was immediately picked up from the electrolyte, rinsed with ultrapure water and finally, the disk was dried. The electrodeposition of PbO<sub>2</sub> onto a Ti/TiO<sub>2</sub>-nanotubes disk array was achieved using a galvanostatic method by using a solution of 0.25M Pb(NO<sub>3</sub>)<sub>2</sub> + 0.1 M HNO<sub>3</sub> by applying 30 mA cm<sup>-2</sup> during 10 min at 25 °C (see Fig. S2 (ESI)). No gas bubbling was involved.

### Surface characterization

Surface morphology of Ti/TiO<sub>2</sub>-nanotubes and Ti/TiO<sub>2</sub>-nanotubes/PbO<sub>2</sub> deposits were characterized using a scanning electron microscope (SEM, TESCAN VEGA model LSU at a 30 KV acceleration voltage), diffraction electronic spectroscopy (EDS, Shimadzu Electron Probe Microanalyzer EPMA-1720) and atomic force microscopy (AFM), while crystalline phases were determined with an X-ray diffractometer (DRX

Bruker model D8Discover) using Cu K $\alpha$  ( $\lambda=1.54 \text{ \AA}$ ) radiation. Electrochemical measurements were carried out using an AutoLab 302N (Metrohm workstation). For the study of electrochemical characteristics of Ti/TiO<sub>2</sub>-nanotubes/PbO<sub>2</sub> and service life performances, cyclic voltammetry (CV) and polarization measurements of PbO<sub>2</sub> deposits were performed in 1.0 mol L<sup>-1</sup> H<sub>2</sub>SO<sub>4</sub> between 0.5 and 3.5 V vs. Ag/AgCl (3M) at 50 mV s<sup>-1</sup>.

### Electrochemical experiments

After that, electrocatalytic features of Ti/TiO<sub>2</sub>-nanotubes/PbO<sub>2</sub> electrode were tested during the EO of dye solution by applying 20, 40 and 60 mA cm<sup>-2</sup> of current density. EO experiments were made by using an electrolytic flow cell with a single compartment with parallel plate electrodes for treating 2 L of 250 mg L<sup>-1</sup> of Acid Blue 113 dye (AB 113) at 25 °C (see Fig S3). The dye was obtained from a textile industry at Santiago de Chile (Chile) and with no further purification for use. The characteristics of the dye Acid Blue 113 are shown in Table 1. Colour and chemical oxygen demand (COD) analyses were performed to evaluate the depollution performances. Also, samples of anolyte were subjected to GC-MS analysis using GC-FOCUS and MS-ISQ Thermo Scientific to identify the intermediates.

### Results and Discussion

Ti/TiO<sub>2</sub>-nanotubes were successfully synthesized in solution of glycerol and ultrapure water containing with NaF and Na<sub>2</sub>SO<sub>4</sub> by galvanostatic electrolysis with a potential of 30 V for 120 min. Surface morphology of deposits was observed by SEM, showing TiO<sub>2</sub> nanotubes with diameters of approximately 100-200 nm as observed in the images.

The TiO<sub>2</sub> nanotubes grow vertically on the substrate and form a dense array, as shown in Fig. 1. Also, EDS measurements were carried out at different spots along the TiO<sub>2</sub> nanotubes, and the typical EDS spectrum is shown in Fig. 1b. The composition analysis shows that the stoichiometry Ti/O corresponds to TiO<sub>2</sub>, which demonstrates that the nanotubes were synthesized. Meanwhile, AFM study reveals the profile of lateral view of TiO<sub>2</sub> nanotubes (see Fig. S4), confirming the nanometric diameter of tubes formed (see Fig. 1). On the other hand, PbO<sub>2</sub> crystals were successfully deposited onto Ti/TiO<sub>2</sub>-nanotubes arrays, according to the Fig. 2. Deposit was composed of orderly arranged tetragonal PbO<sub>2</sub> crystals with sizes that can achieve about 15 μm (see, inset and Fig. 2). These tetragonal crystals can organize in tree form when the electrodeposition time is increased (see Fig. S5 (ESI)). Fig. S6 (ESI) shows clearly the grown of PbO<sub>2</sub> crystals onto TiO<sub>2</sub> nanotubes after 30 min of electrodeposition time. For this reason, the electrolysis time of 10 min is very important to obtain homogenous PbO<sub>2</sub> deposit. The side lengths of PbO<sub>2</sub> are about 3.0-4.0 μm, and the thicknesses of film was minimums as shown in the inset in Fig. 2. EDS measurements were carried out at different spots along the PbO<sub>2</sub> film, and the typical EDS spectrum is shown in Fig. 2. The additional composition analysis showed that the crystals formed in the TiO<sub>2</sub>-nanotubes arrays consist of pure PbO<sub>2</sub>. Fig. S7 (ESI) shows the XRD pattern of the synthesized PbO<sub>2</sub> crystals. All peaks can be indexed to β-PbO<sub>2</sub> phases. No peaks of any other phases or impurities were detected, which also revealed that the pure PbO<sub>2</sub> was obtained. The formation mechanism of PbO<sub>2</sub> morphology during electrodeposition is discussed in ESI. Herein the performances of large TiO<sub>2</sub>-nanotubes/PbO<sub>2</sub> anode for EO were studied (see Fig. S8). Nevertheless, the preliminary examination was performed by CVs of TiO<sub>2</sub>-nanotubes/PbO<sub>2</sub> (shown in Fig. 2) recorded at 50 mV s<sup>-1</sup> in 1.0 M H<sub>2</sub>SO<sub>4</sub>, shown in Fig. 3. In each case, the 20<sup>th</sup> cycle sweeping from 0.0 V to 2.0 V is shown in Fig. 3. In the

negative scanning, a slight reduction signal is observed at about 1.4 V for the PbO<sub>2</sub> deposit, and they can be attributed to the electroreduction of PbO<sub>2</sub> to PbSO<sub>4</sub> via the following electrochemical reaction:  $\text{PbO}_{2(s)} + \text{HSO}_{4(aq)} + 3\text{H}^+ + 2\text{e}^- \rightarrow \text{PbSO}_{4(s)} + 2\text{H}_2\text{O}$ . From the area under the cathodic signal, it can be clearly observed that the charge passed at the Ti/TiO<sub>2</sub>-nanotubes/PbO<sub>2</sub> is several times minor than that of Pb/PbO<sub>2</sub> even when both anodes was treated by similar Pb deposition procedure.

On the reverse scan, only relatively small anodic signals are observed for both samples as shown in Fig. 3, suggesting the well-known passivating effect of PbSO<sub>4</sub>. After several CV curves, the cathodic signal will be smaller in the next cycle because of less availability of PbO<sub>2</sub> for electroreduction. After 40 cycles, the charge passed at the Ti/TiO<sub>2</sub>-nanotubes/PbO<sub>2</sub> is about 50 times minor than that passed at Pb/PbO<sub>2</sub> electrode as shown in inset Fig. 3. Therefore, Ti/TiO<sub>2</sub>-nanotubes/PbO<sub>2</sub> show much better electrochemical properties than Pb/PbO<sub>2</sub> anode, and this may be attributed to the much larger surface area of the TiO<sub>2</sub> nanostructures, giving the much more open-edge morphologies and the much larger network structures to PbO<sub>2</sub> crystals formed. Fig. 3b also shows linear polarization curves of a Pb/PbO<sub>2</sub> and Ti/TiO<sub>2</sub>-nanotubes/PbO<sub>2</sub> electrodes obtained in 1.0 M H<sub>2</sub>SO<sub>4</sub> with a scan rate of 50 mV s<sup>-1</sup>. The curves are very different and show that oxygen evolution potential increases from 0.0 V to 2.8 V versus Ag/AgCl (3.0 M) for Pb/PbO<sub>2</sub> and Ti/TiO<sub>2</sub>-nanotubes/PbO<sub>2</sub>, respectively. This means that Pb/PbO<sub>2</sub> has high oxygen evolution overpotential and consequently is poor electrocatalysts for the oxygen evolution reaction (o.e.r.), however, the potential of o.e.r. was shifted to more positive potential when Ti/TiO<sub>2</sub>-nanotubes/PbO<sub>2</sub> was employed and consequently, disfavoring noticeably the production of oxygen.<sup>33,34</sup> This behavior indicates that the later anode could exhibit good electrocatalytic properties for EO of organic pollutants in solution.<sup>31,33,34</sup>

EO experiments were performed in order to evaluate the electrocatalytic features of disk Ti/TiO<sub>2</sub>-nanotubes/PbO<sub>2</sub> to remove the organic load and color of a dye synthetic effluent with an electrochemical flow cell by applying 20, 40 and 60 mA cm<sup>-2</sup>. Fig. 4 shows color decay during the galvanostatic electrolysis of dye solutions containing 250 mg dm<sup>-3</sup> AB 113. The removal changes were reasonably rapid; indicating that during the first treatment stages there are mechanisms involving dye oxidation to other simpler organics.<sup>33</sup> Oxidation of this complex molecule can result in formation of many intermediates by elimination of chromophore groups prior to production of aliphatic carboxylic acids and carbon dioxide.<sup>34,35</sup> This can be explained because at Ti/TiO<sub>2</sub>-nanotubes/PbO<sub>2</sub> electrodes, •OH radicals formed by water oxidation ( $\text{H}_2\text{O} \rightarrow \bullet\text{OH} + \text{H}^+ + \text{e}^-$ ) can be either electrochemically oxidized to dioxygen ( $\bullet\text{OH} \rightarrow \frac{1}{2} \text{O}_2 + \text{H}^+ + \text{e}^-$ ) or contribute to the complete oxidation of the organic compounds, in this case, dyes ( $\text{Dyes} + \bullet\text{OH} \rightarrow \text{CO}_2 + \text{H}_2\text{O}$ ).<sup>36,37</sup> According to Comninellis,<sup>38</sup> this anode can be classified as non-active anode thus favoring the electrochemical combustion of organic pollutants. However, color removal decreased when an increase on current density was achieved. This behavior is due to the promotion of oxygen evolution reaction<sup>37,38</sup> when an increase in the applied current density was attained. It can be also confirmed by the polarization curves that demonstrated the higher production of oxygen at higher current values (see Fig. 3b). Nevertheless, % of COD values (ESI) clearly demonstrated the oxidation power of this non-active electrode independent on applied current density, at different electrolysis times (see inset in Fig. 4). This outcome is in agreement with data reported by other authors for the anodic oxidation of dyes.<sup>33,39-42</sup> During the electrolysis of synthetic dye effluent, the energy consumption (ESI) seems to be proportional to the applied current density. For example, it increases from 39.2 to 70.3 kWh per m<sup>-3</sup> of effluent treated when the current density passes from 20 to 60 mA cm<sup>-2</sup>. Conversely,

higher energy requirements were needed when Pb/PbO<sub>2</sub> was used as anode (57 to 100 kWh m<sup>-3</sup>). After the EO of synthetic dye using Ti/TiO<sub>2</sub>-nanotubes/PbO<sub>2</sub> anode, by-products were identified by GC/MS. 1-Naphthalenol; naphthalene, 1,6-dimethyl-4-(1-methylethyl) and dibutyl phthalate were identified as intermediates, confirming the chromophore group cleavage as first step and the formation of aromatic intermediates, giving lower coloration to the solution.<sup>41,42</sup> The electrochemical stability of the disk Ti/TiO<sub>2</sub>-nanotubes/PbO<sub>2</sub> was examined by subjecting an electrode to fixed current density measurements for prolonged electrolysis times. Fig. S9 (ESI) shows the variation of E<sub>appl</sub> as a function of time. As revealed from these data, there is almost no increase in the values of E<sub>appl</sub> up to 120 h. Therefore, the disk Ti/TiO<sub>2</sub>-nanotubes/PbO<sub>2</sub> composed of orderly arranged tetragonal PbO<sub>2</sub> crystals showed high electrochemical stability for long-term applications. In addition, it is important to indicate that, no pollution of Pb<sup>2+</sup> was detected after longer times of electrolysis with Ti/TiO<sub>2</sub>-nanotubes/PbO<sub>2</sub> anode, in contrast with the results achieved when Pb/PbO<sub>2</sub> electrode is used. The release of Pb<sup>2+</sup> was monitored by electroanalytical measurements,<sup>43</sup> however, other techniques, such as ICP/MS and ICP/OES,<sup>44-46</sup> can be used to evaluate this parameter.

## Conclusions

In summary, the large PbO<sub>2</sub> electrodes composed of orderly arranged TiO<sub>2</sub> nanotubes were firstly synthesized via a simple, rapid, and efficient electrochemical approach. Compared with Pb/PbO<sub>2</sub> electrodes, this prepared Ti/TiO<sub>2</sub>-nanotubes/PbO<sub>2</sub> can promote the remarkable enhancement in the performances of electrocatalytic materials for treatment of wastewaters.<sup>39,40</sup> The higher electrochemical activities of Ti/TiO<sub>2</sub>-nanotubes/PbO<sub>2</sub> than those of Pb/PbO<sub>2</sub> may be attributed to the larger surface area,

more open-edge morphologies and larger network structures in the crystal body. This study will open a new approach in the search for new metal oxide structures from preparation of TiO<sub>2</sub> nanotubes, giving more stability to non-active anodes for the electrochemical devices with excellent performances.

### Notes and references

† Electronic Supplementary Information (ESI) available: See DOI: 10.1039/c000000x/

- 1 X. Li, D. Pletcher and F. C. Walsh. *Chem. Soc. Rev.*, 2011, **40**, 3879.
- 2 D. Pletcher and F. C. Walsh, *Industrial Electrochemistry*, 2nd ed., Chapman and Hall (London) 1990.
- 3 G. Planté, *Compt. Rend.*, 1859, **49**, 402; G. Planté, *Compt. Rend.*, 1860, **50**, 640.
- 4 A. M. Couper, D. Pletcher and F. C. Walsh, *Chem. Rev.*, 1990, **90**, 837.
- 5 A. J. Bard, R. Parsons and J. Jordan, *Standard Potentials in Aqueous Solutions*, Marcel Dekker, Inc. (New York) 1985.
- 6 A. T. Kuhn, *The Electrochemistry of Lead*, 1st ed. Academic Press Inc. (London) Ltd., 1979.
- 7 D. W. Wabner, R. Huss, F. Hindelang, H. P. Fritz and D. Missol, *Z. Naturforsch.*, 1976, 31B, 45–50.
- 8 D. W. Wabner, H. P. Fritz and R. Huss, *Chem. Ing. Tech.*, 1977, **49**, 329.
- 9 Ch. Comninellis and E. Plattner, *J. Appl. Electrochem.*, 1982, **12**, 399.
- 10 D. Devilliers, M. T. D. Thi, E. Mahe and Q. Le Xuan, *Electrochim. Acta*, 2003, **48**, 4301.

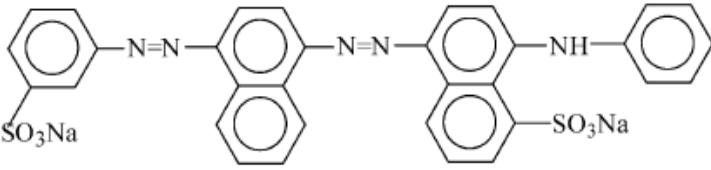
- 11 M. Ueda, A. Watanabe, T. Kameyama, Y. Matsumoto, M. Sekimoto and T. Shimamune, *J. Appl. Electrochem.*, 1995, **25**, 817.
- 12 F. Hine, M. Yasuda, T. Iida, Y. Ogata and K. Hara, *Electrochim. Acta*, 1984, **29**, 1447.
- 13 G. Cao, *Nanostructures & Nanomaterials: Synthesis, Properties & Applications*, Imperial College Press (London) 2004.
- 14 G. A. Ozin and A.C. Arsenault, *Nanochemistry: A Chemical Approach to Nanomaterials*, Royal Society of Chemistry (Cambridge) 2005.
- 15 R. Inguanta, S. Piazza and C. Sunseri, *J. Electrochem. Soc.*, 2008, **155**, K205.
- 16 P. Perret, T. Brousse, D. Be' langer and D. Guay, *J. Electrochem. Soc.*, 2009, **156**, A645.
- 17 P. N. Bartlett, T. Dunford and M. A. Ghanem, *J. Mater. Chem.*, 2002, **12**, 3130.
- 18 A. El Ruby Mohamed, S. Rohani, *Energy Environ. Sci.*, 2011, **4**, 1065.
- 19 Y. L. Pang, S. Lim, H. C. Ong and W. T. Chong, *Applied Catalysis A: General*, 2014, **481**, 127.
- 20 D. Kowalski, D. Kim and P. Schmuki, *Nano Today*, 2013, **8**, 235.
- 21 N.K. Shrestha, P. Schmuki, R.G. Compton and J.D. Wadhawan, *Electrochemistry at TiO<sub>2</sub> nanotubes and other semiconductor nanostructures*, Electrochemistry, RSC Publishing (Cambridge) 2014, **12**, 87-131.
- 22 S. Bauer, S. Kleber and P. Schmuki, *Electrochem. Commun.*, 2006, **8**, 1321.
- 23 M. Assefpour-Dezfuly, C. Vlachos and E.H. Andrews, *J. Mater. Sci.*, 1984, **19**, 3626.
- 24 J.M. Macak, H. Tsuchiya and P. Schmuki, *Angew. Chem. Int. Ed.*, 2005, **44**, 2100.

- 25 R.P. Antony, T. Mathews, C. Ramesh, N. Murugesan, A. Dasgupta, S. Dhara, S. Dash and A.K. Tyagi, *Int. J. Hydrogen Energy*, 2012, **37**, 8268.
- 26 D. Gong, C.A. Grimes, O.K. Varghese, W. Hu, R.S. Singh, Z. Chen and E.C. Dickey, *J. Mater. Res.*, 2001, **16**, 3331.
- 27 S. Sreekantan, Z. Lockman, R. Hazan, M. Tasbihi, L.K. Tong and A.R. Mohamed, *J. Alloys Compd.*, 2009, **485**, 478.
- 28 N. Pugazhenthiran, S. Murugesan and S. Anandan, *J. Hazard. Mater.*, 2013, **263**, 541.
- 29 M. Plodinec, A. Gajovic, G. Jaksa, K. Zagar and M. Ceh, *J. Alloys Compd.*, 2014, **591**, 147.
- 30 Y. Tang, Z. Jiang, Q. Tay, J. Deng, Y. Lai, D. Gong, Z. Dong and Z. Chen, *RSC Adv.*, 2012, **2**, 9406.
- 31 C.A. Martínez-Huitle and M. Panizza, *Application of PbO<sub>2</sub> Anodes for wastewater Treatment*, In: *Advances in Chemistry Research: Applied Electrochemistry*, Nova Science Publishers, Inc. (New York) 2010, 269-300.
- 32 M. Cerro-López, Y. Meas-Vong, M.A. Méndez-Rojas, C.A. Martínez-Huitle and M.A. Quiroz, *Appl. Catal. B: Environ.*, 2014, **144**, 174.
- 33 C. A. Martínez-Huitle and E. Brillas, *Appl. Catal., B.*, 2009, **87**, 105.
- 34 C. A. Martínez-Huitle and S. Ferro, *Chem. Soc. Rev.*, 2006, **35**, 1324.
- 35 M. Panizza and G. Cerisola, *Chem. Rev.*, 2009, **109**, 6541.
- 36 B. Marselli, J. García-Gómez, P.-A. Michaud, M.A. Rodrigo and Ch. Comninellis, *J. Electrochem. Soc.*, 2003, **150**, D79.
- 37 Ch. Comninellis, *Electrochim. Acta.*, 1994, **39**, 1857.
- 38 Ch. Comninellis, A. Kapalka, S. Malato, S.A. Parsons, I. Poullos and D.Mantzavinos, *J. Chemical Technol. Biotechnol.*, 2008, **83**, 769.

- 39 M. Panizza and G. Cerisola, *Appl. Catal. B: Environ.*, 2007, **75**, 95.
- 40 E. Brillas and C.A. Martínez-Huitle, *Appl. Catal. B Environ.*, 2015, **166-167**, 603.
- 41 C.K.C. Araújo, G.R. Oliveira, N.S. Fernandes, C.L.P.S. Zanta, S.S.L. Castro, D.R. da Silva and C.A. Martínez-Huitle, *Environ. Sci. Pollut. Res.* 2014, **21**, 9777.
- 42 J.H. Bezerra Rocha, M.M. Soares Gomes, E.V. dos Santos, E.C. Martins de Moura, D. Ribeiro da Silva, M.A. Quiroz and C.A. Martínez-Huitle, *Electrochim. Acta.* 2014, **140**, 419.
- 43 M.M.S.G. Eiband, K.C.A. Trindade, K. Gama, J.V. Melo, C.A. Martínez-Huitle and S. Ferro, *J. Electroanal. Chem.*, 2014, **717-718**, 213.
- 44 H. Lin, J. Niu, J. Xu, H. Huang, D. Li, Z. Yue and C. Feng, *Environ. Sci. Technol.*, 2013, **47**, 13039.
- 45 J. Niu, H. Lin, J. Xu, H. Wu and Y. Li, *Environ. Sci. Technol.*, 2012, **46**, 10191.
- 46 H. Lin, J. Niu, S. Ding and L. Zhang, *Water Res.*, 2012, **46**, 2281.

## Tables

**Table 1.** The characteristics of Acid Blue 113 (AB 113).

Formula	$C_{32}H_{21}N_5Na_2O_6S_2$
Azo dye	C.I. Acid Blue 113
IUPAC name	Disodium 8-anilino-5-[[4-(3-sulfonatophenyl)azo-1-naphthyl] azo] naphthalene-1-sulfonate
$\lambda_{max}$	570 nm
MW	681.66
CI	26360
Chemical structure	

## Figures

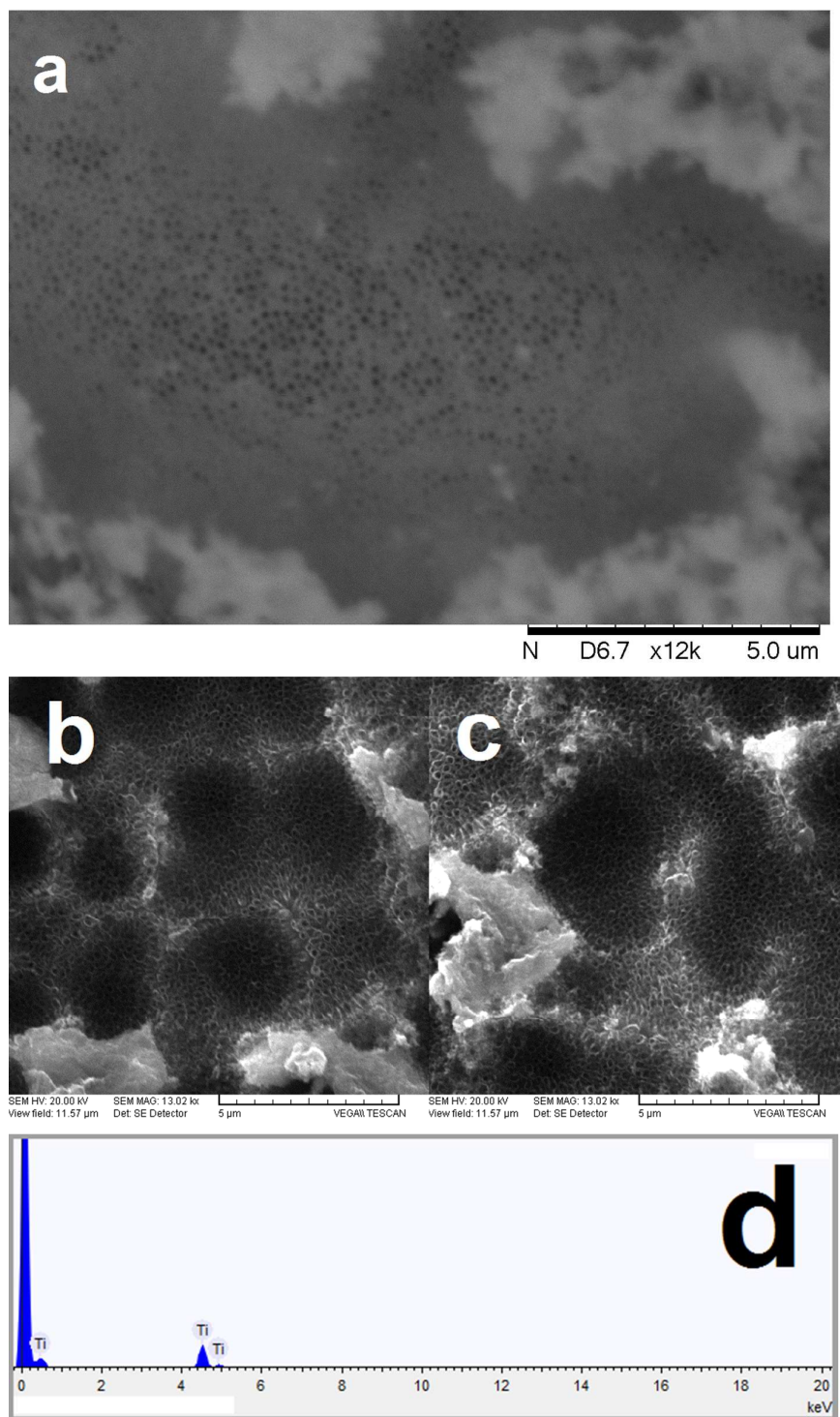


Fig. 1. (a) SEM image of anodized Ti/TiO<sub>2</sub>-nanotubes. The inset (b) and (c) are the SEM images of the magnified orderly arranged nanotubes. (d) EDS spectrum regarding the composition analysis, showing that it corresponds to TiO<sub>2</sub>.

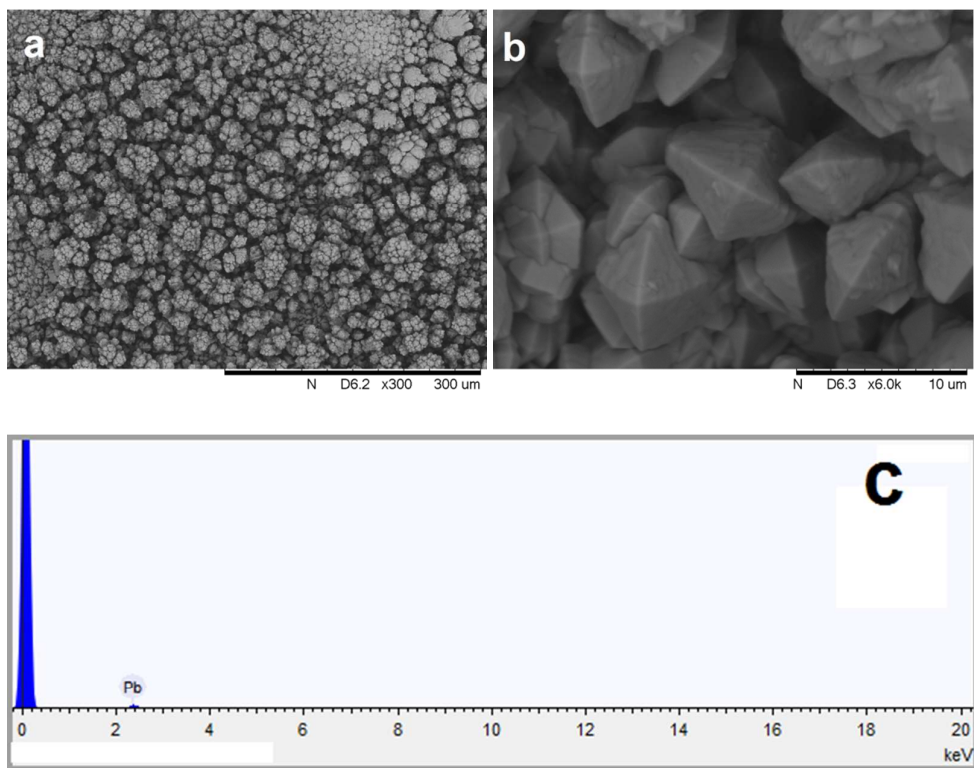


Fig. 2. (a) SEM images of PbO<sub>2</sub> deposit into Ti/TiO<sub>2</sub>-nanotubes and the magnified orderly arranged PbO<sub>2</sub>-tetragonal crystals. (c) EDS spectrum regarding the composition analysis, showing that the thin film corresponds to PbO<sub>2</sub>.

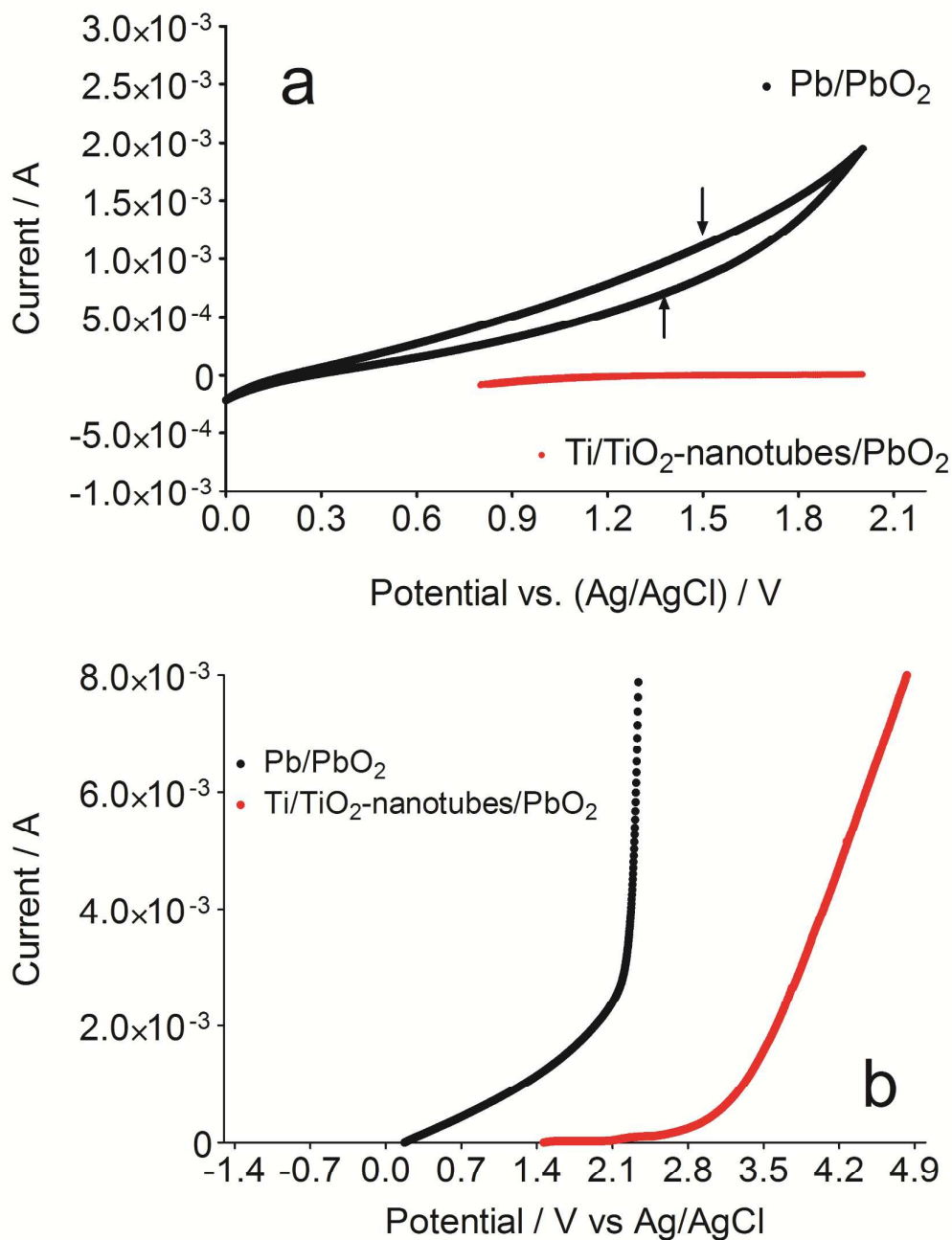


Fig. 3. Electrochemical measurements obtained in  $\text{H}_2\text{SO}_4$ : a) CV curves of  $\text{PbO}_2$  (black curve) and  $\text{Ti/TiO}_2\text{-nanotubes/PbO}_2$  (red curve) anodes, with  $2 \text{ cm}^2$  of geometrical area. Inset: Magnification of CV curve for  $\text{Ti/TiO}_2\text{-nanotubes/PbO}_2$  electrode. b) Polarization curves for both electrodes.

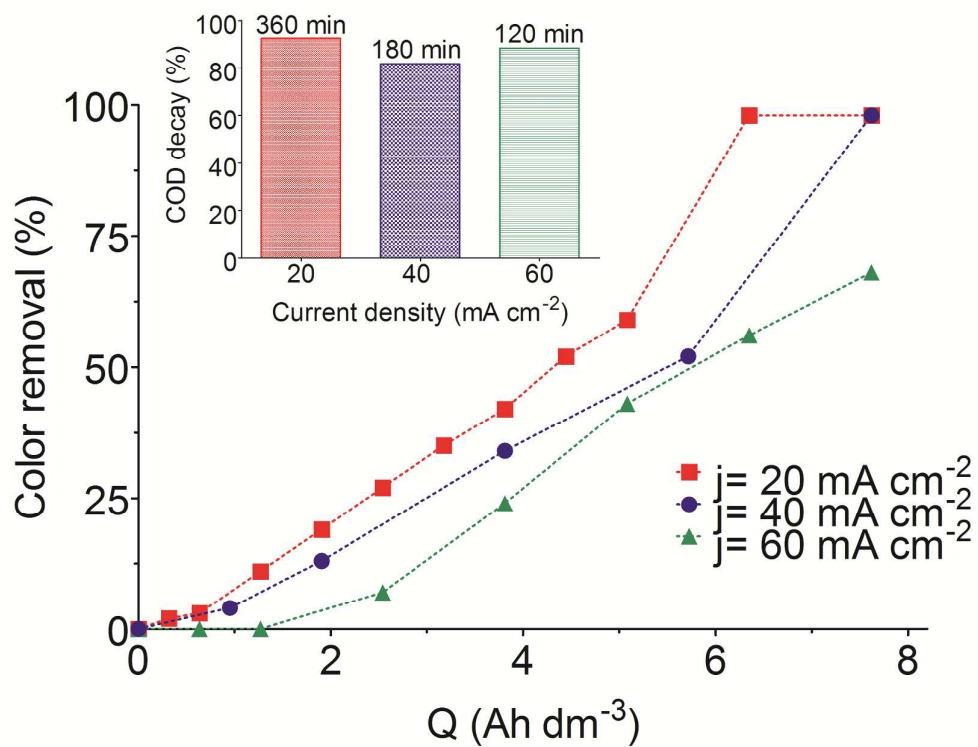


Fig. 4. Electrochemical treatment of synthetic dye effluent using a disk Ti/TiO<sub>2</sub>-nanotubes/PbO<sub>2</sub> anode with 65 cm<sup>2</sup> of geometrical area by using electrochemical flow cell. Color decay, as a function of electrical charge passed, by applying different current densities. The inset is the percentage of COD removal, as a function of applied current density.